

## HYDROGEOLOGICAL CHARACTERIZATION OF THE AQUIFERS OF THE SALITRE REGION THROUGH STABLE ISOTOPES ( $\delta D$ AND $\delta^{18}O$ ) AND GEOCHEMISTRY

Christian Pereira Lopes dos Santos<sup>1</sup>, Luiz Rogério Bastos Leal<sup>2</sup>, Antonio Expedito Gomes de Azevedo<sup>3</sup>,  
Maria do Rosário Zucchi<sup>3</sup> and Alan Robert Dutton<sup>4</sup>

**ABSTRACT.** The important aquifers of the Salitre basin are encompassed within the geological framework of the metasedimentary rocks of the Chapada Diamantina Group and in the carbonate rocks of the Una Group and Caatinga Formation. For fifty five water samples from carbonate aquifers,  $\delta D$  values varied from  $-43\text{‰}$  to  $-10\text{‰}$ , and  $\delta^{18}O$  values from  $-5.9\text{‰}$  to  $-3.3\text{‰}$ , with high concentrations of dissolved total salts. The variability allowed us to discern three process of salinization: i) samples with more negative isotope values are produced primarily by transpiration and/or dissolution in the evaporitic rocks; ii) samples with less negative isotopic values indicate that evaporation is predominant; and iii) samples from metasedimentary aquifers, with low concentrations of dissolved total salts and  $\delta D$  values ranging from  $-36\text{‰}$  to  $-20\text{‰}$  and  $\delta^{18}O$  values from  $-5.4\text{‰}$  to  $-3.5\text{‰}$  indicated low evaporation. The piezometric map indicated that the groundwater flow flux is from both the east and west towards the center of the basin and that the general direction of surface water flux is from south to north, where the water level is closer to the surface.

**Keywords:** carbonate rocks, semiarid region, hydrochemistry, stable isotopes, karst aquifers.

**RESUMO.** Os aquíferos importantes da bacia do Salitre estão abrangidos dentro do arcabouço geológico metassedimentares do Grupo Chapada Diamantina e nas rochas carbonáticas do Grupo Una e da Formação Caatinga. Para cinquenta e cinco amostras de água dos aquíferos carbonatados, os valores de  $\delta D$  variaram de  $-43\text{‰}$  a  $-10\text{‰}$  e os valores de  $\delta^{18}O$  de  $-5,9\text{‰}$  a  $-3,3\text{‰}$ , com altas concentrações de sais totais dissolvidos. A variabilidade indica três processos de salinização: i) amostras com mais valores de isótopos negativos são produzidas primariamente por transpiração e/ou dissolução nas rochas evaporíticas; ii) amostras com menos valores isotópicos negativos indicam que a evaporação é predominante; e iii) amostras de aquíferos metassedimentares, com baixas concentrações de sais totais dissolvidos e valores de D variando de  $-36\text{‰}$  a  $-20\text{‰}$  e valores de  $\delta^{18}O$  de  $-5,4\text{‰}$  a  $-3,5\text{‰}$  indicaram pouca evaporação. O mapa piezométrico indicou que o fluxo subterrâneo é tanto do leste quanto do oeste em direção ao centro da bacia e que a direção geral do fluxo de superfície é do sul para o norte, onde o nível freático está mais próximo da superfície.

**Palavras-chave:** rochas carbonáticas, região semiárida, hidroquímica, isótopos estáveis, aquíferos cársticos.

---

Corresponding author: Maria do Rosário Zucchi

<sup>1</sup>Instituto Federal de Educação Ciência e Tecnologia Baiano, Campus Catu, Rua Barão de Camaçari, 118, Centro, 48110-000, Catu, BA, Brazil – E-mail: cplsgs@gmail.com

<sup>2</sup>Universidade Federal da Bahia, Instituto de Geociências, Campus Universitário de Ondina, Ondina, 40170-115, Salvador, BA, Brazil – E-mail: Irogerio@ufba.br

<sup>3</sup>Universidade Federal da Bahia, Pós-Graduação em Geofísica, Rua Barão de Geremoabo, S/N Federação, 40050-090, Salvador, BA, Brazil – E-mails: expedito@ufba.br, mrzucchi@ufba.br

<sup>4</sup>University of Texas at San Antonio, Department of Earth and Environmental Sciences, 6900 N, Loop 1604 W, San Antonio, TX 78249-0663 – E-mail: alan.dutton@utsa.edu

## INTRODUCTION

The Salitre region is among the poorest regions in northeastern Brazil (Fig. 1). The rural and urban populations of the area depend largely on water from aquifers and from ephemeral rivers, which is also used for irrigation and small industrial activities. However, little surface water is available, and the waters are highly saline, especially during certain seasons (Martins, 1986; Bastos Leal et al., 2005; Lima et al., 2005; Santos, 2008). As a result, people in the region are subject to a seasonal shortage of potable water and rely heavily on groundwater. The pressure to find new sources of freshwater has been increasing over the last 10 years due to growth in the population and areas under irrigation, as well as the initiation of new mineral industries. This has caused frequent conflicts over water among intensive agriculture, industry and domestic use (Bastos Leal et al., 2005; Brito et al., 2005).

In recent years, several aquifers in Bahia State have been studied according to the framework of the National Council of Scientific and Technologic Development (CNPq) and the Center for Research in Geophysics and Geology at the Universidade Federal da Bahia, Brazil (CPGG-UFBA) to improve the knowledge of these aquifers and increase the water supply. The first detailed hydrogeological study in the Salitre region included fieldwork in the summers of 2004 and 2005 (Lima et al., 2005; Santos, 2008). The applied methods include hydrogeological mapping, geophysical investigation, hydrochemical and isotopic sampling and analyses. To improve the management of these aquifers using scientific rather than political criteria, more investigation is needed.

Hydrochemical and environmental isotope techniques have been increasingly applied to water resource management and can help provide a better understanding of the aquifer recharge, dissolution of minerals within the bedrocks, water mixing and evaporation process, and spring discharge. In addition, they are essential for defining groundwater hydrodynamic models (Clark & Fritz, 1997; Thomas & Rose, 2003; Marfia et al., 2004; Shanyengana et al., 2004; Barbieri et al., 2005).

The main goals of this study are: a) to analyze geological features, hydrochemistry and stable isotopes ( $^{18}O$  and  $D$ ) to understand the recharge, salinization and possible mixing processes of groundwater; and b) to develop a conceptual hydrogeological model of the aquifer system. The results of this work will improve our understanding of both the hydrogeological dynamics of the aquifers in the Salitre basin and the process of water resource management and protection. They will also offer an assessment of the quality of water for human, irrigation and industrial uses.

## GEOGRAPHICAL AND CLIMATIC OVERVIEW

The study area is located in the northeastern region of Brazil in the semiarid climate zone, and includes a catchment of approximately 14,500 km<sup>2</sup>. The Salitre river and its tributaries form the principal drainage network of the study area. The morphology of the region is largely dependent on the geological structure, which includes elevations of approximately 1,200 m above sea level in the siliciclastic rocks of Chapada Diamantina Group. The elevations are between 500 and 600 m in carbonatic sequence rock outcroppings in the central part of the basin, and the minimum elevation is approximately 400 m, in the northern region where the Salitre basin is bounded by the São Francisco river valley (Fig. 1).

The mean annual precipitation in the Salitre region ranges from approximately 450-500 mm/yr. The dry season is between June and January, but in the south of the region, the precipitation can reach 1000 mm/yr. Average annual temperature is 26°C, and daily temperatures range between 18°C and 38°C and the potential evapotranspiration demand is between 1700-2200 mm/yr (Martins, 1986).

This semiarid region of Brazil has an interannual variation in climatic conditions, with some years experiencing extremely dry summers where water deficits can range from 100 mm/yr in the south to over 1,700 mm/yr in the drier north (Martins, 1986). In these climatic conditions, evaporation is important in controlling the chemical signature of groundwater. However, the different composition of the rocks in this region and the occurrence of soluble minerals (ex: calcite, dolomite, gypsum) can provide another source of the ions dissolved in groundwater. (Ettayfi et al., 2012; Sánchez et al., 2015; Salles et al., 2019).

## GEOLOGICAL AND HYDROGEOLOGICAL FRAMEWORK

The oldest geologic unit, representing 3% of the surface of the study area, is formed by an Archean-Paleoproterozoic granite-gnaiss complex and supracrustal rocks located in the extreme north of the basin (Fig. 1). These oldest rocks are covered by Mesoproterozoic sedimentary rocks represented by the Chapada Diamantina Group, which forms a QPC (Quartzit-Pelite-Carbonate) association. The covering layer comprises distinct metaconglomerate, metasandstone and metacarbonate lithofacies associated with alluvial fan, fluvial, desertic tidal flat, deltaic and marine depositional systems (Pedreira, 1997). There are economically important deposits of iron and sulfides associated with this QPC sequence.

The Neoproterozoic sequence of the Una Group overlies the Mesoproterozoic rocks of the Chapada Diamantina. It consists

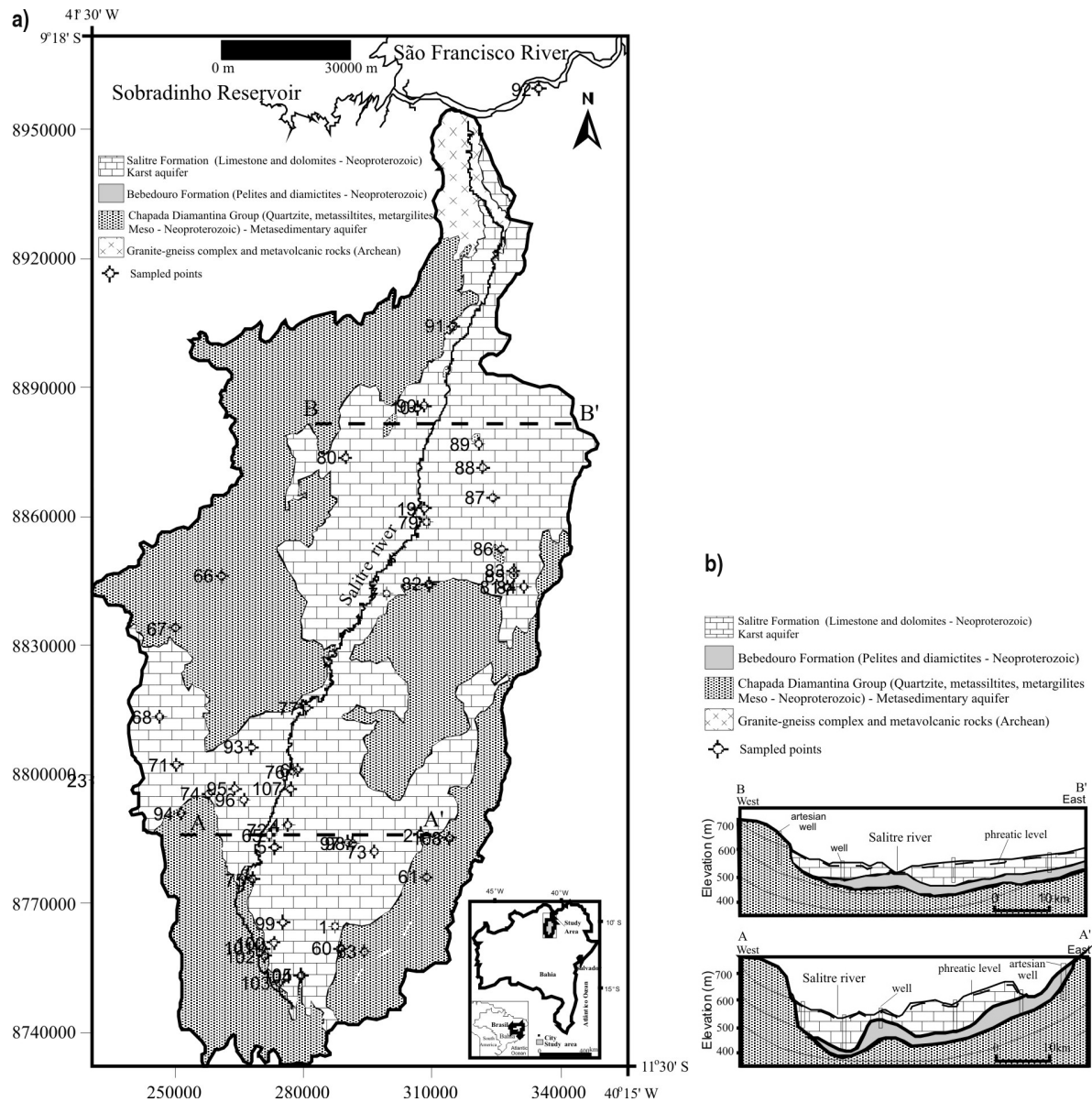


**Figure 1** – a) Location of study area and distribution of carbonatic (karst) sequences in Bahia, Brazil and Geological / Hydrogeological domains of the Salitre watershed; b) Hydrogeologic cross-section along transect in the south (A-A') and north (B-B') of the basin.

of the diamictite and pelites of the Bebedouro Formation at the base, followed by the predominantly marine carbonates of the Salitre Formation (Fig. 1). Carbonate sequences of the Salitre Formation are well exposed in the study area and its correlative units in the Bambuí Group have been part of an extensive Neoproterozoic platform (>300,000 km<sup>2</sup>), with sedimentation commencing during the transgression sea over much of the São Francisco Craton between 600 and 670 Ma (Misi & Kyle, 1994; Misi & Veizer, 1998).

The carbonatic sequence is formed by succession sedimentary lithofacies composed (from bottom to top) by argillaceous dolostone, laminated dolomitic limestone, evaporitic limestone, marl, oolitic limestone and black limestone resulting from the two transgressive-regressive cycles. The most economically important contents are the host phosphatic stromatolites and Pb-Zn sulfide mineralizations associated with stratiform and stratbound pyrite, spharelite and galene in the associated with the dolomitic limestone layers (Misi & Kyle,

1994; Misi & Veizer, 1998). On the other hand, geomorphological and isotopic studies of  $\delta^{34}S$  in the carbonatic rocks in the north of the Salitre region show that cave development was mostly caused by sulfuric acid dissolution due to pyrite oxidation during the Tertiary period (Auler, 1999).

The present structural configuration of the Salitre basin, which is formed of a large syncline cuted by fracture systems and flexural folds in the northeastern segment, was developed during a collision related to Brasiliano/Pan African tectonic cycle about 650-500 Ma (Lagoeiro, 1990; Brito Neves et al., 1999) (Fig. 1). The man aligned faults and fractures, mostly NNE-SSW, along the Salitre river strike may represent basement structures that were reactivated during carbonatic sedimentation (Alvarenga & Dardenne, 1978). In the vadose zone these structures act as infiltration pathways for the recharge of deep aquifers, and they are a major flow channel within the saturated zone.

The main aquifers in the Salitre watershed are represented by rocks of the Chapada Diamantina Group, which form a confined, fractured aquifer that occupies 46% of the basin and by the carbonatic sequence of the Salitre Formation, which is a unconfined karst aquifer that occupies approximately 51% of the basin and creates the majors reservoir in the study area. The rocks of the Bebedouro Formation act as an aquitard between the aquifer systems (Fig. 1). The groundwater flow is generally controlled by topography and faults, and it is congruent with the major rivers and their tributaries.

The recharge of the Chapada Diamantina fractured aquifer occurs by rainfall in the high mountains. More than 90% of the wells currently pump less than 30 m<sup>3</sup>/h, and in phreatic conditions the water table is 20 m below the surface.

Figure 2 shows the groundwater elevation contours from Salitre watershed. These maps indicate that groundwater flow goes from the east and west to the center of the watersheds and that the general direction of surface flow is from south to north where the phreatic level in the aquifer is closer to the surface.

Geophysical electrical resistivity studies in the karst aquifer show that it has thickness ranges from 70 m in the north segment to 250 m in the south (Lima et al., 2005). The karst aquifer has allogenic groundwater recharge associated with cross-formational flow from underlying Mesoproterozoic siliciclastic rocks in the low mountains surrounding the karst basin and autogenic recharge in the central region of the aquifer associated with tectonic and karst structures (fractures, sinkhole, vertical shafts and conduits). There is no perennial surface

drainage on the carbonatic rocks. The only perennial river drains from the Chapada Diamantina Group's rocks and undergoes diffuse infiltration into the karst aquifer.

The principal discharge zone from the aquifer is the Pacuí Spring, with a discharge of 0.23 m<sup>3</sup>/s as measured in January 1994 (Auler, 1999). Well productivity in the karst aquifer ranges from 1 to 50 m<sup>3</sup>/h, and approximately 50% of the wells present pumping less than 10 m<sup>3</sup>/h. However, in the region of the aquifer where the karstification is more developed and in discharge zones, the pumping rates can be as high as 150 m<sup>3</sup>/h (Bastos Leal et al., 2005).

## SAMPLES AND ANALYTICAL PROCEDURES

Seven superficial water and forty-nine groundwater samples were collected from wells and a spring associated with the karst (41 samples) and fractured (8 samples) aquifers and from drainage during the months of November 2004 and 2005. The water for major cation and anion analyses was stored in 1000-ml high-density polyethylene bottles with no headspace, filtered through 0.45  $\mu$ m Millipore filters, acidified with nitric acid (cations only) to pH < 2 before bottling and then refrigerated. The multi-parameter instrument (Horiba U-50 series) automatically records temperature, pH and electrical conductivity of water in situ, with resolutions of 0.1°C, 0.01 pH and 1  $\mu$ s/cm, respectively. Cation chemistry was determined by inductively coupled plasma (precision,  $\pm 1\%$ ) and anions were analyzed by ion chromatography (precision,  $\pm 1\%$ ). The total dissolved solids (TDS) were calculated by summing concentrations of major ions.

For stable isotope determinations, a 50-ml glass bottle was filled and the oxygen and hydrogen isotopes were measured using a mass spectrometer, model DELTA PLUS (TermoFinnigan). Oxygen isotope ratios were determined by the CO<sub>2</sub> equilibration method with precision of  $\pm 0.1$  ‰. (Epstein & Mayeda, 1953). Hydrogen isotope ratios were determined by Cr-reduction method (Brand et al., 2000) with precision of  $\pm 1$  ‰. Both  $\delta D$  and  $\delta^{18}O$  measurements were standardized using Vienna Standard Mean Ocean Water (VSMOW).

## RESULTS AND DISCUSSION

Sampling locations, well data and analytical results are presented in Tables A1 and A2 in the Appendix.

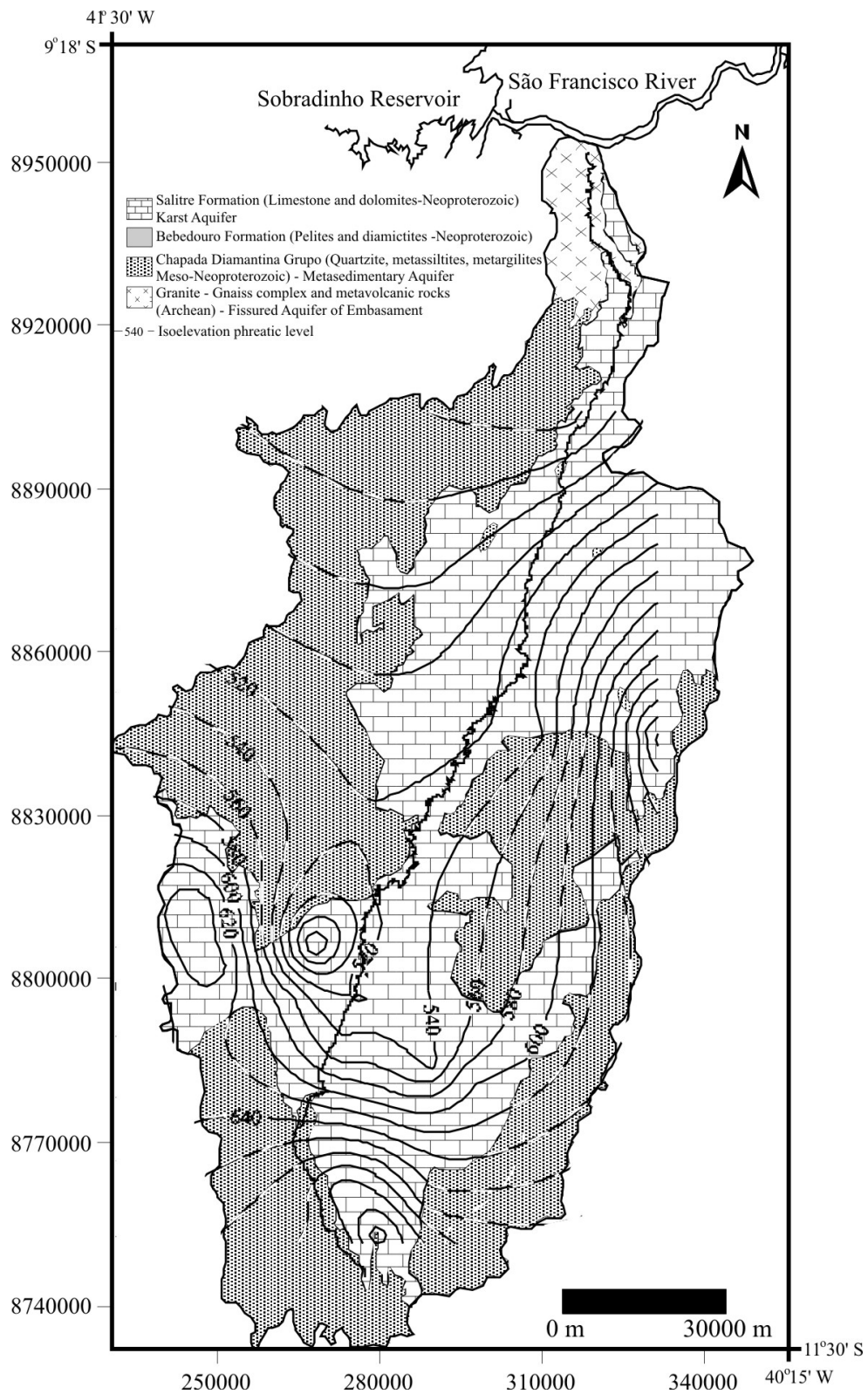


Figure 2 – Groundwater elevation contours of the Salitre watershed.

## CHEMICAL COMPOSITION

The groundwater samples showed the occurrence of two different hydrochemical groups. In the fractured aquifer, the total dissolved solids (TDS) ranged from 108 mg/l to 334 mg/l, but locally exceeded 1,500 mg/l (sample TCM-67). This was reflected by the electrical conductivity (EC) values of the samples, which varied from 222 to 600  $\mu S/cm$ , except in sample TCM-67, which had a value of 1,800  $\mu S/cm$  (Table A1). The water samples from the karst aquifer were characterized by higher total mineralization, ranging from 578 mg/l (sample TCK-07) to 3,236 mg/l (sample TCK-60). The EC of these samples was also higher and varied from 900 to 4,800  $\mu S/cm$ , which was consistent with the higher salinity of the karst groundwater (Table A1). All of the water samples were acid to slightly alkaline. Their pH indices were uniform and ranged between 6.0 and 7.6 (Table A1). The temperatures of groundwater samples measured in the field were between 26°C and 29°C.

Ca and Mg ions were the dominant cations in samples from the metasedimentary aquifer and their concentrations varied widely, while  $HCO_3^-$  was a dominant anion, except in sample TCM-67, which had  $SO_4$  as its dominant anion (Table A1). The Ca content ranged from 27 mg/l (sample TCM-03) to 295 mg/l (sample TCM-67). The Mg content was between 17 mg/l (sample TCM-03) and 101 mg/l (sample TCM-67). The concentration of  $HCO_3^-$  ranged from 97 mg/l (sample TCM-66) to approximately 231 mg/l (sample TCM-10). These ion compositions placed the water from the fractured aquifer in a Ca-Mg- $HCO_3^-$  type (Fig. 3). The normal content of  $SO_4$  ion ranged from 3.4 to approximately 24 mg/l, but in sample TCM-67 it was 1,188 mg/l, indicating a Ca- $SO_4$  composition type for this water sample. Cl and Ca ions are dominant in the samples from the karst aquifer. Thus, the waters were of Ca-Cl type (Fig. 3). The Ca content ranged from 66 to 354 mg/l, and Cl from 63 to 1,300 mg/l (Table A1). The Mg content varied from 31 to 94 mg/l, and the  $SO_4$  from 22 to 158 mg/l. The  $HCO_3^-$  content varied from 110 to 447 mg/l while  $NO_3^-$  content ranged from 1.5 to 19 mg/l. The contents of K and Na varies from 4.1 to 28 mg/l and from 88 to 308 mg/l, respectively. The content of these elements in the waters from the karst aquifer was higher than in those from the fissured aquifer (Table A1).

Slightly elevated nitrate concentrations, which were above the limits set for human use (10 mg/l; MS 2914) were found in several samples in the karst aquifer (ex. TCK-70 and TCK-74; Table A1), suggesting contamination derived from pollution sources such as domestic effluents, septic tanks, and waste from an unlined municipal-landfill in the region.

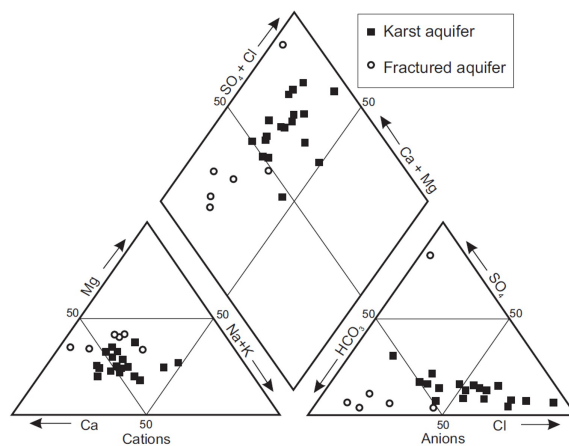


**Figure 3** – Piper diagram showing the ionic composition of samples in Salitre watershed; circle samples from fractured aquifer and square samples from karst aquifer.

In the Mg vs Ca plot, it is apparent that the karst aquifer contains significantly more calcium and magnesium than fissured aquifer, which reflects the predominant rock type. The concentrations increase during the underground flow, which can be explained by additional mineral dissolution and mixing processes within the aquifers (Fig. 4a). This behavior can also be observed in the strong correlation between these ions and TDS in both aquifers (Figs. 4b and 4c).

The high Ca and Mg content observed in sample TCM-67, which was collected in the metasedimentary aquifer, most likely result from the dissolution of the carbonate rocks of the Caboclo Formation that is associated with the Chapada Diamantina Group (Pedreira, 1997). In contrast, some authors explain the higher  $SO_4$  concentration in groundwater (e.g., Hem, 1992; Motyka et al., 2005; Charideh & Rahman, 2007) suggest that the high concentration of sulfate ions can originate from infiltration of water that is enriched in  $SO_4$  by pollution, pyrite oxidation or dissolution of evaporate rocks. However, in the region where this sample was collected, there are no industrial activities, important urban occupation or occurrence of the evaporate rocks, but on the other hand the occurrences of the sulfured mineral associated with the Chapada Diamantina Group and Salitre Formation (Pedreira, 1994; Misi & Veizer, 1998). This suggests that the high content of sulfate in sample TCM-67 is most likely associated with the dissolution of sulfured minerals (ex: pyrite) that occurs in these parts of the Chapada Diamantina Group.

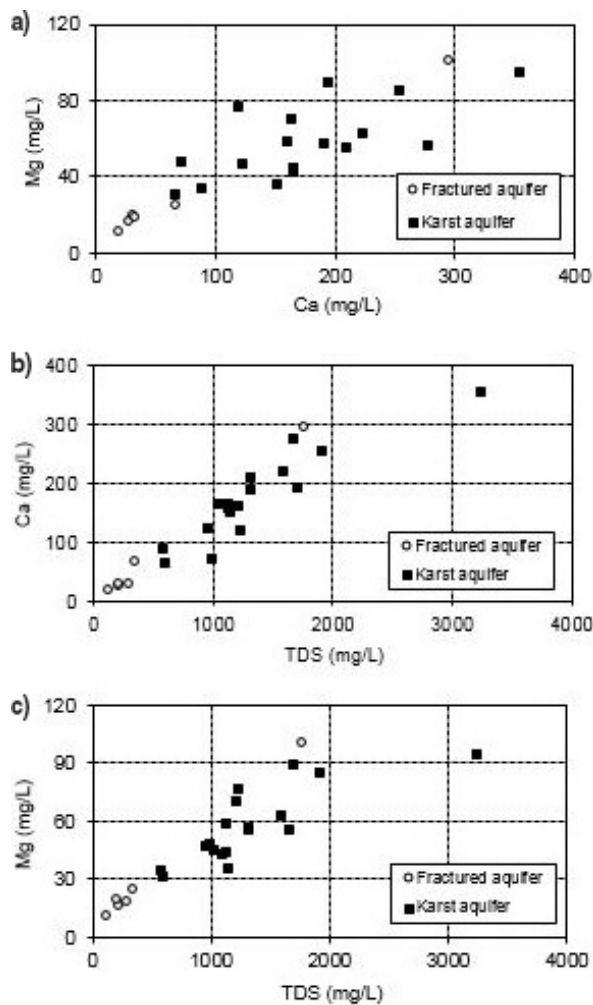


**Figure 4** – The relationship among ions and total dissolved salts in groundwater of the Salitre watershed: a) magnesium and calcium; b) magnesium and total dissolved salt; and c) calcium and total dissolved salt.

The relationship between Cl and the major cations Na, Ca and Mg (Fig. 5) indicate that there is no mixing between the groundwater of these aquifers. The lowest Cl concentrations in the fractured aquifer reflect water recharge from the high altitudes and regional rainwater, with possible enrichment by evaporation processes. The highest Cl concentrations are associated with the karst aquifer and are derived mainly from the evaporation processes, as originally suggested by Bastos Leal et al. (2005), Santos (2008).

The plots of Cl/SO<sub>4</sub> versus SO<sub>4</sub> ion in both aquifers show a negative slope, where the concentrations of dissolved sulfate and chloride ions are inversely related, especially in karst groundwater (Fig. 6). This higher concentrations of sulfate in the

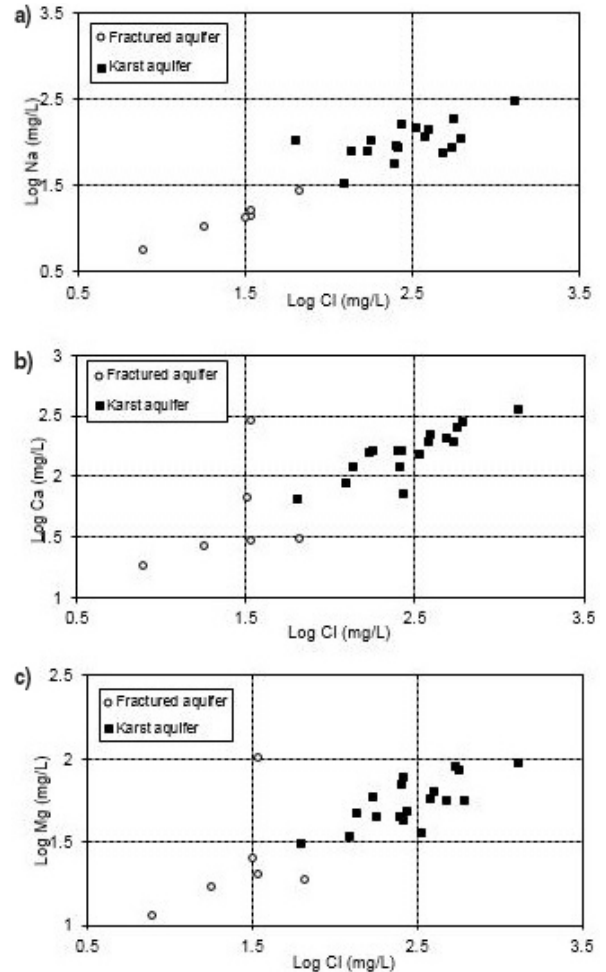


**Figure 5** – Relationships between major ions: a) sodium and chloride; b) calcium and chloride; and c) magnesium and chloride in groundwater of the Salitre watershed.

groundwater of the karst aquifer indicates a gypsum dissolution and/or oxidation of pyrite, as suggested by Guerra (1986) and noted by Valle & Karmann (2005) while studying the Una karst in the Irecê region. The relative scatter of the data most likely reflects the evaporative concentration of sulfate associated with reactions within the bedrock.

The importance of evaporative concentration, is also demonstrated by the Na/Cl ratios of the groundwater samples, which varied from 0.41 and 0.73 in fractured aquifer samples and between 0.15 and 0.59 in the samples from the karst aquifer, except in the sample TCK-04, in which the ratio was 1.67 (Fig. 7). This range and the negative slope of the data imply that chloride also enters the karst groundwater from rain. Additionally, the

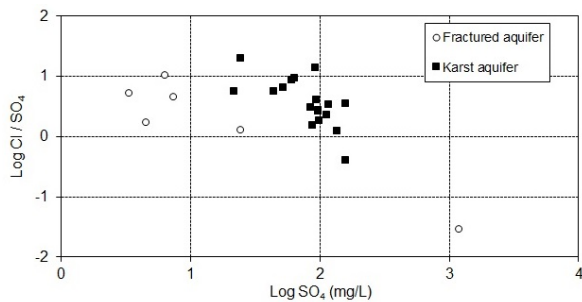


**Figure 6** – Relationship between the Cl<sup>-</sup>/SO<sub>4</sub><sup>2-</sup> ratio and SO<sub>4</sub><sup>2-</sup> concentration in groundwater of the Salitre watershed.

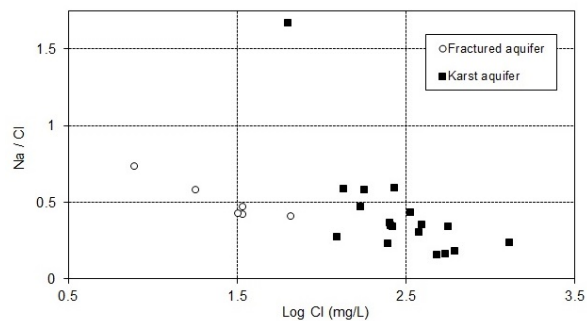


**Figure 7** – Relationship between the sodium/chloride ratio and chloride concentration in groundwater of the Salitre watershed.

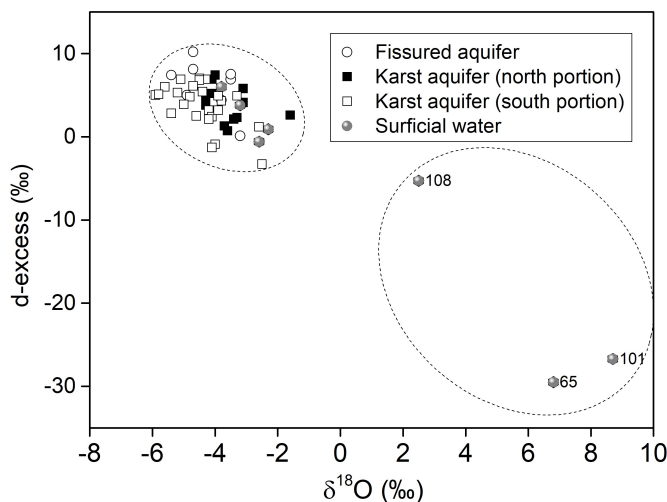


**Figure 8** – *d*-excess versus  $\delta^{18}O$  for surface water and groundwater in the Salitre watershed.

variation in the cation-anion proportion within each system can be explained by differences in residence time and the degree of rock-water interaction.

### STABLE ISOTOPE GEOCHEMISTRY

The stable isotopes of oxygen and hydrogen are generally considered to be transported conservatively in shallow aquifers, due to the prevalence of high rock-water ratios and an absence of significant evaporation. However, in the case of the Salitre basin, with its high temperatures (mean 26° C) and evaporation (1700-2200 mm/year), it is likely that rainfall evaporates before and even after infiltration occurs. Therefore, the isotopic signatures should be combined with other fingerprints to evaluate the level of interaction between groundwater and soluble minerals and the salinization process.

The isotopic composition of the dam water in the study region was highly enriched by evaporation, with  $\delta^{18}O$  ranging from 2.5 to 8.7 ‰ and  $\delta D$  from 15 to 43 ‰ (Table A2). On the other hand, the isotopic compositions of the spring and Salitre river water basin are relatively depleted in stable isotopes, -1.6 to -3.8 ‰ for  $\delta^{18}O$  and -10 to -26 ‰ for  $\delta D$ . Figure 8 shows diagram *d*-excess versus  $\delta^{18}O$ . In this diagram almost surficial water and groundwater samples are closer together, except for surficial water 108, 101 and 65 means that evaporation enrichment isotopic has occurred.

The groundwater of the fissured aquifer ranged from -3.2 to -5.4 ‰ for  $\delta^{18}O$  and from -20 to -36 ‰ for  $\delta D$  (Table A2). According to the isotopic composition, the karst groundwater samples were divided in two groups. The first group consisted of the groundwater from the south the Salitre basin and presented

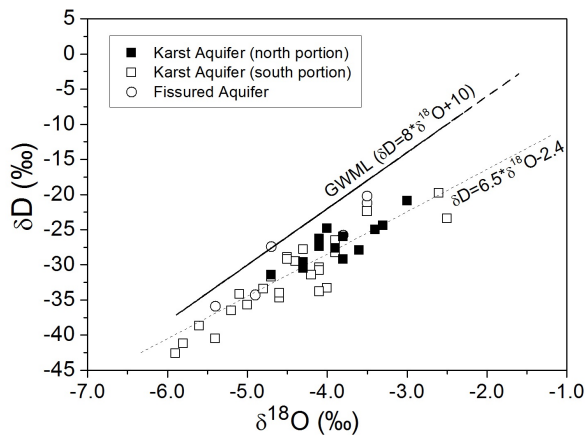


Figure 9 –  $\delta D$  versus  $\delta^{18}O$  for groundwater in the Salitre watershed.

large variation in the isotopic composition, with  $\delta^{18}O$  ranging between -2.5 and -5.9 ‰ while the  $\delta D$  ranged between -20 and -43 ‰. In the second group, groundwater from north area of the region, isotopes varied less and the enrichment, -3.1 to -4.7 ‰ for  $\delta^{18}O$  and -19 to -31 ‰ for  $\delta D$ , suggests more evaporation in this part of the Salitre basin (Table A2).

The plot of all the groundwater isotope data on the  $\delta^{18}O$ - $\delta D$  diagram shows a line below the GWML ( $\delta D = 6.5 * \delta^{18}O - 2.4$ ), suggesting that evaporation has enriched the water in heavy isotopes (Fig. 9). Additionally, the relationship between  $\delta^{18}O$  and  $\delta D$  in groundwater from the fissured and karst aquifers indicate the same hydrological origin for both and that recharge occurs during the major rainy season.

Similar indicated in the relationship between Cl and the major cations (Na, Ca and Mg), the Cl- $\delta^{18}O$  relationship reveals that the karst groundwater group has elevated salinity with relatively narrow isotopic enrichment (Fig. 10). This confirms that the primary cause of the salinity in the groundwater of the karst aquifer is its interaction with the carbonatic sequence and the secondary cause is evaporation. In contrast, the narrow Cl variation of groundwater from the fissured aquifer, and its increased  $\delta^{18}O$  confirm an acute evaporation process in the Salitre watershed.

Figure 11 shows isolines of deuterium concentrations created by a kriging interpolation in SURFER software. This map shows that water samples from the south of the basin are isotopic depleted, while in the north they are enriched in heavy isotopes. This trend is related to the hydric balance as seen in the piezometric map of the basin, with higher precipitation, lower

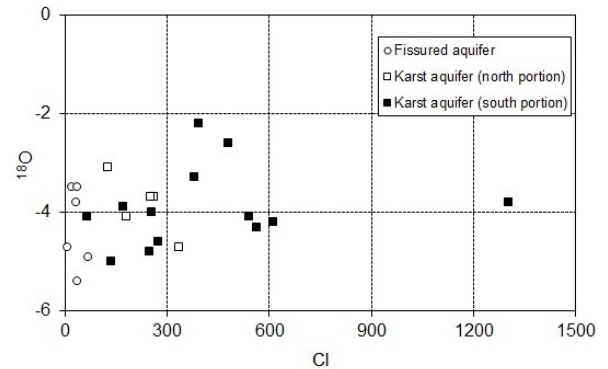


Figure 10 – Relationship between  $\delta^{18}O$  and Cl in the groundwater of the Salitre watershed.

evaporation and greater depths of the phreatic level in the south and lower precipitation, higher evaporation and shallow phreatic levels in the north.

## CONCLUSION

The groundwaters that recharge the drainage axis of the Salitre river are a mix of precipitation collected in the metasedimentary rocks of the Chapada Diamantina Group and water that circulates through the carbonate rocks of the Salitre karst aquifer.

The chemical and isotopic data show that the main drivers of salinity in the region are evaporation and secondarily chemical interactions with the carbonate rocks.

The hydrological budget of Salitre basin, which has about 500 mm/year of precipitation and potential evapotranspiration of more than 2000 mm/year, defines the basin as semiarid. The recharge of the aquifers is therefore a result of precipitation that escapes the intense evaporation and is collected in fractures and joints.

Only in surface water, such as in dams, is evaporation dominant and able to cause enrichment in heavy isotopes and dissolved salts.

In samples from wells close to the river and from wells where the aquifer has a shallow open surface, there was  $^{18}O$  and D enrichment due to evaporation.

For samples from the karstic aquifer, which have high salinity and low D and  $^{18}O$  values, transpiration is the dominant process. Transpiration leaves behind the salts without isotopic fractionation.

Through analyses of the piezometric lines, the depth of the phreatic level and the deuterium maps, it was possible to

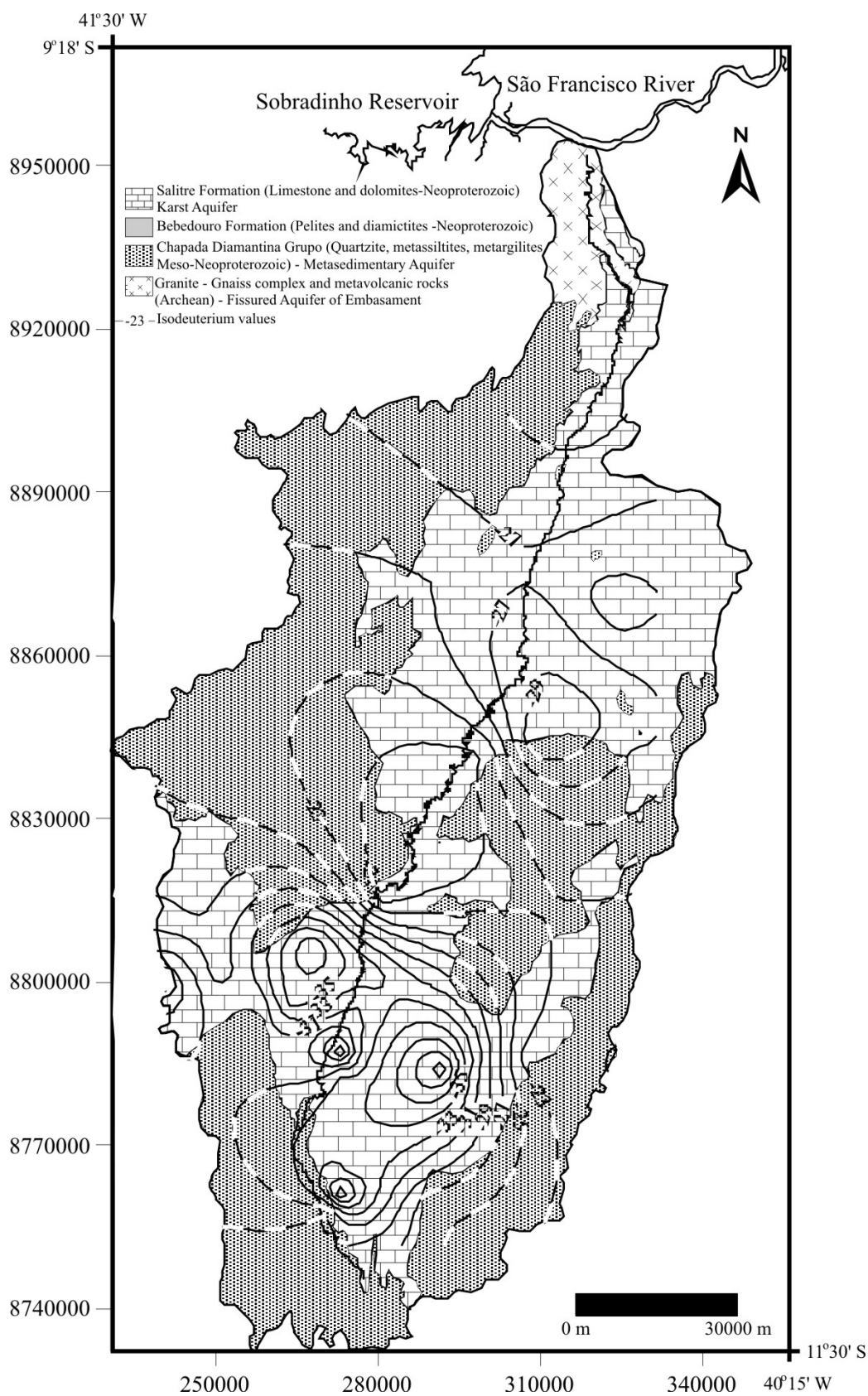


Figure 11 – Isocontour deuterium map of groundwater in the Salitre watershed.

understand that the underground flow is from east and west toward the center of the basin, and the it generally flows from south to north. The water in the north part of the basin is more enriched in heavy isotopes and dissolved salts.

The results of this work contribute to a better understanding of the hydrogeological dynamics that underlie water quality as evaluated for human, irrigation and industrial use.

## ACKNOWLEDGMENTS

The authors thank the Conselho Nacional de Desenvolvimento Científico e Tecnológico – CNPq (National Council of Scientific and Technologic Development – Process No. 475655/03-6) and Coordenação de Aperfeiçoamento de Pessoal de Nível Superior, Brazil - CAPES (Process No. 518/05 and BEX-0030/06-6) for financial support of the present work, as well as international cooperation between the Universidade Federal da Bahia and University of Texas at San Antonio.

## REFERENCES

ALVARENGA CJS & DARDENNE MA. 1978. Geology of Bambuí and Paranoá Groups on the Serra de São Domingos, Minas Gerais, Brazil. In: Proceedings of XXX Cong. Bras. Geol. Recife, PE, Brazil. August 1978, 2: 546-556. [in Portuguese].

AULER AS. 1999. Karst evolution and paleoclimate of eastern Brazil. PhD Thesis, University of Bristol, England. 268 pp.

BARBIERI M, BOSCHETTI T, PETITTA M & TALLINI M. 2005. Stable isotope ( $^2\text{H}$ ,  $^{18}\text{O}$  and  $^{87}\text{Sr}/^{86}\text{Sr}$ ) and hydrochemistry monitoring for groundwater hydrodynamics analysis in a karst aquifer (Gran Sasso, Central Italy). *J. Appl. Geochem.*, 20: 2063-2081.

BASTOS LEAL LR, SILVA HM, LUZ JAG & LIMA OAL. 2005. Hydrogeology of karst aquifers on the São Francisco Craton, Bahia State. Implications for management of groundwater. In: III Simp. Craton do São Francisco. Short Paper, Salvador, BA, Brazil. October 2005. p. 370-372. [in Portuguese].

BRAND WA, AVAK H, SEEDORF R, HOFMANN D & CONRADI T. 2000. New methods for fully automated isotope ratio determination from hydrogen at the natural abundance level. *Geophys. Prospect.*, 28: 967-976.

BRITO LTL, SRINIVASAN VS, SILVA AS, GHEYI HR, GALVÃO CO & HERMES LC. 2005. Influence of anthropic activities on water quality of Salitre river basin. *Rev. Bras. Eng. Agrícola e Ambiental*, 9(4): 596-602. [in Portuguese].

BRITO NEVES BB, CAMPOS NETO MC & FUCK RA. 1999. From Rodinia to Western Gondwana: an approach to the Brasiliano-Pan African Cycle and orogenic collage. *Epis. J. Intern. Geosc.*, 22(3): 155-166.

CHARIDEH A & RAHMAN A. 2007. Environmental isotopic and hydrochemical study of water in the karst aquifer and submarine springs of the Syrian coast. *Hydrogeology Journal*, 15(2): 351-364.

CLARK ID & FRITZ P. 1997. *Environmental isotopes in Hydrogeology*. Lewis, New York, 311 pp.

EPSTEIN S & MAYEDA TK. 1953. Variation of the  $^{18}\text{O}/^{16}\text{O}$  ratio in natural waters. *Geochem. et Cosm. Acta*, 4: 213-224.

ETTAYFI N, BOUCHAOU L, MICHELOT JL, TAGMA T, WARNER N, BOUTALEB S, MASSAULT M, LGOURNA Z & VENGOSH A. 2012. Geochemical and isotopic (oxygen, hydrogen, carbon, strontium) constraints for the origin, salinity, and residence time of groundwater from a carbonate aquifer in the Western Anti-Atlas Mountains, Morocco. *Journal of Hydrology*, 438-439: 97-111.

GUERRA AM. 1986. Karstification process and hydrogeology of Bambuí Group on Irecê Region, Bahia. PhD Thesis, Universidade de São Paulo. SP, Brazil, 267 pp. [in Portuguese].

HEM JD. 1992. Study and interpretation of the chemical characteristics of natural water. United States Geological Survey, Water-Supply Paper 2254: 263 pp.

LAGOIEIRO LE. 1990. Study of deformation of the Una Group carbonatic sequence on the Irecê region, Bahia. MSc. Thesis, Universidade Federal de Ouro Preto, MG, Brazil, 165 pp. [in Portuguese].

LIMA OAL, BASTOS LEAL LR & LUZ JAG. 2005. Geology and geophysics characteristics of the aquifers on Salitre basin, Bahia State. In: III Simp. Craton do São Francisco. Short Paper, Salvador, BA, Brazil. October 2005, p. 366-369. [in Portuguese].

MARFIA AM, KRISHNAMURTHY RV, ATEKWANA EA & PANTON WF. 2004. Isotopic and geochemical evolution of ground and surface waters in karst dominated geological setting: a case study from Belize, Central America. *J. Appl. Geochem.*, 19: 937-946.

MARTINS MR. 1986. Evaluation of water resources on the watershed of the Bahia State, Salitre watershed. Governo do Estado da Bahia. Publicação Especial. Centro de Estatística e Informação, v.1, 101 pp. Salvador, BA, Brazil. [in Portuguese].

MISI A & KYLE JR. 1994. Upper Proterozoic carbonate stratigraphy, diagenesis, and stromatolitic phosphorite formation, Irecê Basin, Bahia, Brazil. *J. Sediment. Res.*, 64: 299-310.

MISI A & VEIZER J. 1998. Neoproterozoic carbonate sequences of the Una Group, Irecê Basin, Brazil: chemostratigraphy, age and correlations. *Precamb. Res.*, 89: 87-100.

MOTYKA J, GRADZINSKI M, BELLA P & HOLÚBEK P. 2005. Chemistry of waters from selected caves in Slovakia – a reconnaissance study. *Environ. Geol.*, 48: 682-692.

- PEDREIRA AJ. 1994. The Espinhaço Supergroup in the Center-Eastern Chapada Diamantina, Bahia State: Sedimentology, Stratigraphy and Tectonics. PhD Thesis, Universidade de São Paulo. SP, Brazil. 126 pp. [in Portuguese].
- PEDREIRA AJ. 1997. Depositional systems in the Chapada Diamantina Sequence, Centro Oriental, Bahia. *Rev. Bras. Geoc.*, 27(3): 229-240. [in Portuguese].
- SALLES LQ, BASTOS LEAL LR, PEREIRA RGFA, LAUREANO FV, NASCIMENTO SAM, ZUCCHI MR & BARBOSA NS. 2019. Hydrogeochemical and isotopic tools ( $\delta^{18}O$  and  $\delta^2H$ ) applied to understanding the processes of groundwater salinization in Proterozoic carbonate aquifers: Evidence from the semi-arid region of northeastern Brazilian. *Anuário Inst. Geoc.*, 42(2): 117-125. [in Portuguese].
- SÁNCHEZ D, BARBERÁ JA, MUDARRA M & ANDREO B. 2015. Hydrogeochemical tools applied to the study of carbonate aquifers: examples from some karst systems of Southern Spain. *Environ. Earth Sci.*, 74: 199-215.
- SANTOS CPL. 2008. Analysis of salinization processes of the waters of the Salitre river basin by environmental tracers. PhD Thesis on Geophysics, Universidade Federal da Bahia. BA, Brazil. 105 pp. [in Portuguese].
- SHANYENGANA ES, SEELY MK & SANDERSON RD. 2004. Major-ion chemistry and ground-water salinization in ephemeral floodplains in some arid regions of Namibia. *J. Arid. Environ.*, 57: 211-223.
- THOMAS J & ROSE T. 2003. Environmental isotopes in Hydrogeology. *Environ. Geol.*, 43(5): 532.
- VALLE MA & KARMANN I. 2005. Hydrochemical of Una Group in the Irecê basin, Bahia State: An example of acid sulfur action in karst system. In: III Simp. Craton do São Francisco. Short Paper, Salvador, BA, Brazil. October 2005, p. 377-380. [in Portuguese].

Recebido em 25 de abril de 2019 / Aceito em 28 de novembro de 2019

Received on April 25, 2019 / Accepted on November 28, 2019

APPENDIX

Table A1 – Chemical composition of groundwater in the Salitre basin of the Bahia State, Brazil.

ID No	Sample	Location	Coordinate		T °C	EC µS/cm	pH	TDS mg/l	Ca mg/l	Mg mg/l	Na mg/l	K mg/l	HCO <sub>3</sub> mg/l	SO <sub>4</sub> mg/l	Cl mg/l	NO <sub>3</sub> mg/l
			Lat. S	Long. W												
<b>Metasedimentary aquifer</b>																
1	TCM-03	Caat. do Moura (aw)	10.9763	40.7027	27.7	334	7.2	206	27	17	10	5	140	3	18	0.2
24	TCM-10	Engenho Pacui (s)	10.1134	40.8169	29.4	600	7.0	334	66	25	14	3	231	25	32	1.3
3	TCM-61	Faz. Lage (w)	11.0673	40.7511	27.0	350	7.2	198	30	20	14	7	140	7	34	0.2
7	TCM-66	Bela (aw)	10.4311	41.1844	27.6	222	6.5	108	18	11	6	7	97	5	8	0.2
8	TCM-67	Lagoa do Anjico (w)	10.5393	41.2838	27.9	1800	6.4	1761	295	101	16	4	206	1188	34	0.6
18	TCM-75	Tabua (aw)	11.0685	41.1231	28.0	500	6.3	289	31	19	27	11	126	6	66	0.6
<b>Karst aquifer</b>																
2	TCK-02	Faz. Bebedouro (w)	10.9763	40.7639	27.9	2100	7.5	1318	190	57	115	7	279	95	379	10.8
5	TCK-05	Pogo Verde (d)	11.0022	41.0755	27.0	1500	7.0	1030	165	45	58	8	291	44	248	9.9
9	TCK-23	Faz. M. Chapéu (w)	10.8573	41.4545	26.4	1500	6.5	1118	159	59	80	5	349	136	170	14.5
10	TCK-70	Lagoa dos 33 (w)	10.8507	41.3779	28.4	1400	7.6	958	122	47	80	4	339	87	136	18.1
11	TCK-71	Faz. Boa Vista (w)	10.8268	41.2839	26.2	2900	6.4	1911	254	85	191	7	327	158	564	15.2
14	TCK-04	Ouroândia (w)	10.9556	41.0468	27.2	1000	6.7	591	66	31	105	6	351	158	63	15.2
16	TCK-73	Faz. São José (w)	11.0124	40.8623	28.5	1800	6.0	1211	163	71	93	4	447	97	253	14.5
17	TCK-74	Faz. Q. Nova (w)	10.8890	41.2153	28.0	2300	6.4	1588	222	63	140	6	331	117	394	19.0
19	TCK-06	Casa Nova (w)	10.9557	41.0257	28.5	1500	7.3	986	72	48	162	9	253	98	272	3.9
20	TCK-76	Casa Nova (w)	10.8428	41.0348	26.8	2400	7.3	1698	194	90	88	8	251	61	540	1.5
21	TCK-77	Pedra Vermelha (w)	10.7091	41.0059	27.9	1700	6.6	1316	210	56	76	10	253	24	481	2.0
22	TCK-07	Lagoa (d)	10.6469	40.8493	26.2	900	6.8	578	89	34	34	5	233	22	124	1.6
25	TCK-80	Patos - I (w)	10.4585	40.5752	29.1	1700	6.9	1084	165	43	89	6	293	85	262	10.9
26	TCK-09	Lagoa Branca (w)	10.2913	40.7514	27.1	1500	6.6	1228	119	77	89	10	311	114	258	13.0
27	TCK-81	Faz. T. da Onça (w)	10.4589	40.5756	28.7	1600	6.7	1120	164	45	104	5	399	99	180	12.9
28	TCK-82	Faz. de Balto (w)	10.4513	40.7424	29.8	1800	6.6	1146	151	36	145	13	271	52	335	9.3
29	TCK-60	Salinas (w)	11.2164	40.9361	28.2	4800	6.4	3236	354	95	308	28	110	93	1302	3.5
30	TCK-01	Morro da Onça (w)	11.1697	40.9472	25.3	2600	7.2	1663	277	56	110	12	186	64	612	5.3

aw – artesian well; w – well; s – spring; d – doline

Table A2 – (to be continued on next page) – Isotopic composition of ground and surface waters in the Salitre basin, Bahia, Brazil.

Sample ID	Coordinate Lat. S	Coordinate Long. W	Type of sample	Depth (m)	Static level (m)	Elev. (m)	Number of samples	$\delta D$ ( $\text{‰} \pm 1\text{‰}$ )	$\delta^{18}O$ ( $\text{‰} \pm 0.1\text{‰}$ )	$d\text{-excess}$ ( $\text{‰}$ )
<b>Surface water</b>										
TC-13	09.53.14	40.38.23	river	-	-	-	1	-18	-2.3	0.9
TC-65	10.58.33	41.05.12	dam	-	-	-	2	25	6.8	-29.5
TC-90	10.04.33	40.45.04	river	-	-	512	1	-25	-3.8	6.0
TC-92	09.54.33	40.41.17	river	-	-	362	1	-21	-2.6	-0.6
TC-94	10.55.46	41.16.24	river	-	-	658	1	-22	-3.2	3.8
TC-101	11.12.52	41.06.10	dam	-	-	704	1	43	8.7	-26.7
TC-108	10.59.06	40.42.06	dam	-	-	677	1	15	2.5	-5.3
<b>Groundwater – karst aquifer (north area)</b>										
TCK-07	10.38.14	40.50.00	doline	-	-	515	2	-20	-3.1	4.1
TCK-08	10.37.09	40.54.13	doline	-	-	-	1	-19	-3.1	5.8
TCK-09	10.17.29	40.45.05	well	80	20.0	-	3	-28	-3.7	1.3
TCK-79	10.19.12	40.44.48	river	-	-	517	1	-10	-1.6	2.6
TCK-80	10.11.02	40.55.08	well	150	52.3	540	1	-25	-4.0	7.4
TCK-81	10.27.32	40.34.32	well	80	3.0	686	1	-27	-4.1	5.2
TCK-82	10.27.05	40.44.33	well	60	15.0	559	1	-31	-4.7	6.1
TCK-83	10.25.23	40.33.32	well	37	12.2	710	1	-28	-3.9	3.2
TCK-84	10.27.26	40.32.25	well	101	4.8	742	1	-26	-4.1	6.9
TCK-85	10.25.59	40.33.44	well	60	10.0	720	1	-30	-4.3	3.8
TCK-86	10.22.42	40.35.15	well	80	11.7	669	1	-28	-3.6	0.7
TCK-87	10.16.10	40.36.20	well	60	15.0	614	1	-25	-3.4	2.1
TCK-88	10.12.22	40.37.36	well	60	6.4	584	1	-24	-3.3	2.3
TCK-89	10.12.23	40.37.37	well	46	9.0	-	1	-26	-3.8	4.3
TCK-91	09.54.33	40.41.17	well	30	5.2	446	1	-30	-4.3	4.5
<b>Groundwater – Karst aquifer (south area)</b>										
TCK-01	11.10.11	40.56.50	well	84	0.0	668	3	-30	-4.2	3.2
TCK-02	10.58.35	40.45.50	well	79	7.0	615	3	-21	-3.3	4.9
TCK-04	10.57.21	41.02.49	well	80	8.0	568	2	-31	-4.1	2.4
TCK-05	11.00.08	41.04.34	doline	-	-	635	3	-33	-4.8	4.8
TCK-06	10.50.21	40.01.33	well	83	10.0	556	3	-34	-4.6	2.5

**Table A2** – (continued from previous page) – Isotopic composition of ground and surface waters in the Salitre basin, Bahia, Brazil.

Sample ID	Coordinate Lat. S	Coordinate Long. W	Type of sample	Depth (m)	Static level (m)	Elev. (m)	Number of samples	$\delta D$ (‰ ± 1‰)	$\delta^{18}O$ (‰ ± 0.1‰)	$d$ -excess (‰)
<b>Groundwater – Karst aquifer (south area)</b>										
TCK-23	10.5127	41.2725	well	110	1.0	586	1	-28	-3.9	3.2
TCK-60	11.1259	40.5610	well	35	11.0	689	1	-26	-3.8	4.3
TCK-68	10.4334	41.1908	well	120	60.0	727	2	-27	-3.9	4.9
TCK-70	10.5104	41.2242	well	130	18.0	-	1	-36	-5	3.9
TCK-71	10.4937	41.1202	well	80	36.0	695	1	-28	-4.3	6.9
TCK-72	10.5755	41.0433	well	80	9.0	560	1	-23	-2.5	-3.3
TCK-73	11.0045	40.5144	well	270	30.0	634	1	-33	-4.0	-0.9
TCK-76	10.5034	41.0205	well	150	8.0	560	1	-34	-4.1	-1.3
TCK-77	10.4233	41.0021	well	33	18.7	555	1	-20	-2.6	1.2
TCK-83	10.4731	41.0725	well	163	19.0	467	1	-39	-5.6	6.0
TCK-95	10.5242	41.0935	well	160	21.0	592	1	-36	-5.2	5.3
TCK-96	10.5406	41.0825	well	157	33.0	-	1	-34	-4.6	2.5
TCK-97	10.5935	40.5508	well	80	60.0	603	1	-41	-5.4	2.8
TCK-98	10.5943	40.5431	well	95	32.0	594	1	-43	-5.9	5.0
TCK-99	10.0937	44.0332	well	90	34.0	740	1	-34	-5.1	6.9
TCK-100	11.1209	41.0442	well	15	4.8	753	1	-41	-5.8	5.1
TCK-102	11.1349	41.0255	well	123	10.7	728	1	-29	-4.4	5.4
TCK-103	11.1713	41.0405	well	70	17.0	738	1	-29	-4.5	7.0
TCK-104	11.1621	40.0116	well	79	14.5	798	1	-29	-4.5	6.8
TCK-105	11.1620	41.0115	doline	-	-	-	1	-32	-4.7	6.1
TCK-107	10.5247	41.0227	well	160	25.8	551	1	-31	-4.2	2.1
<b>Metasedimentary aquifer</b>										
TCM-03	10.5904	40.4209	well	150	0.0	678	3	-21	-3.5	6.9
TCM-10	10.0449	40.4553	spring	-	-	-	1	-26	-3.8	4.4
TCM-12	10.0039	40.4223	well	114	30.0	-	1	-25	-3.2	0.1
TCM-61	11.0402	40.4504	well	80	20.0	757	1	-20	-3.5	7.5
TCM-63	11.1322	40.5306	well	150	11.0	678	1	-29	-4.7	8.1
TCM-66	10.2552	41.1104	well	80	0.0	615	1	-27	-4.7	10.2
TCM-67	10.3221	41.1702	well	-	-	749	1	-36	-5.4	7.4
TCM-75	11.0407	41.0723	well	30	0.0	560	1	-34	-4.9	5.0